Anatomy of Nanoscale Propulsion

Vinita Yadav,[1] Wentao Duan,[1] Peter J. Butler,[2,*] and Ayusman Sen[1,*]

[1]Department of Chemistry and [2]Department of Biomedical Engineering, The Pennsylvania State University, University Park, Pennsylvania 16802; email: pbutler@psu.edu, asen@psu.edu

Annu. Rev. Biophys. 2015. 44:77–100

The *Annual Review of Biophysics* is online at biophys.annualreviews.org

This article's doi: 10.1146/annurev-biophys-060414-034216

*Corresponding authors

Keywords

nanomotors, micromotors, micropumps, enzyme motors, enzyme pumps, electrophoresis, diffusiophoresis, chemotaxis

Abstract

Nature supports multifaceted forms of life. Despite the variety and complexity of these forms, motility remains the epicenter of life. The applicable laws of physics change upon going from macroscales to microscales and nanoscales, which are characterized by low Reynolds number (*Re*). We discuss motion at low *Re* in natural and synthetic systems, along with various propulsion mechanisms, including electrophoresis, electrolyte diffusiophoresis, and nonelectrolyte diffusiophoresis. We also describe the newly uncovered phenomena of motility in non-ATP-driven self-powered enzymes and the directional movement of these enzymes in response to substrate gradients. These enzymes can also be immobilized to function as fluid pumps in response to the presence of their substrates. Finally, we review emergent collective behavior arising from interacting motile species, and we discuss the possible biomedical applications of the synthetic nanobots and microbots.

Contents

INTRODUCTION

Motility is a critical feature of life. The abilities to sense one's environment, to advance toward food and away from toxins, and to communicate are as vital to the survival of a bacterium as they are to that of a blue whale. However, as one goes from macro to micro and ultimately to nano scale, the applicable laws of physics change, necessitating the use of different mechanisms to achieve motility. As size decreases, the ratio of surface area to volume increases, implying that volume-dependent forces (such as inertia), which dominate at longer length scales, become less relevant as objects are scaled down. Instead, surface-dependent forces must be utilized to induce motion (107, 130). This review focuses on motion at the nanoscale and microscale and on the physics that governs this motion.

Reynolds Number

The Reynolds number (*Re*) refers to a dimensionless quantity defined as the ratio of inertial to viscous forces, and this number helps to predict transport properties at different scales:

$$Re = \rho V l/\eta, \qquad 1.$$

where ρ is the density of the fluid, V is the mean velocity relative to the fluid, l is the characteristic linear dimension or the traveled length in the fluid, and η is the dynamic viscosity of the fluid. A low *Re* implies that viscosity is the dominant force, and a high *Re* implies that inertia dominates. Bacteria and other unicellular organisms are the best examples of low *Re* swimmers; for these swimmers, $Re = 10^{-4}$, whereas for an average-sized human being in water, $Re = 10^{4}$. According to the scallop theorem, only nonreciprocal motion can lead to net propulsion in the low-*Re* regime (68). Nonreciprocal motion requires that time-reversal symmetry be broken, for example, by the introduction of the asymmetry in the swimmer design. Although a low *Re* represents the first challenge to nanoscale and microscale motion, this challenge is not the only one.

Brownian Passive Diffusion Versus Directed Motion

At low *Re*, microscale objects are subject to the rapid thermal bumping by solvent molecules, and are driven into motion when collisions are uneven. This effect creates what is known as Brownian diffusion where the objects diffuse and wander around in a solution. Thermal bumping also causes an object to rotate and randomly change orientation, known as Brownian rotation. In contrast, directed motion requires an input of energy.

The translational particle diffusion coefficient, D_t, can be calculated as follows:

$$D_t = k_B T/6\pi\eta a, \quad 2.$$

whereas the rotational particle diffusion coefficient, D_r, is governed by the following equation:

$$D_r = k_B T/(8\pi\eta a^3). \quad 3.$$

In both equations above, k_B is the Boltzmann constant, T is the absolute temperature, η is the viscosity of fluid through which the particle moves, and a is the radius of such a particle.

To examine the nature of particle motion, the mean-squared displacement (MSD) over different time intervals (τ) is calculated by analyzing the trajectories of particles. For several idealized types of motions, the MSD has been shown to increase as a function of τ raised to some power α (Equation 4) (81).

$$\text{MSD} = K\tau^{\alpha} \quad 4.$$

K is a constant with a value that depends on the diffusion coefficient of the particle. For particles undergoing a purely diffusive, two-dimensional random Brownian walk, K is equal to four times the diffusion coefficient of the particles, and the MSD increases linearly with τ (i.e., $\alpha = 1$) (96). Because typical Brownian diffusion is by far the most commonly observed, systems in which α does not equal 1 are often deemed as having anomalous diffusive behavior. Values of α that are greater than 1 correspond to superdiffusive systems, and those that are less than 1 correspond to subdiffusive systems (21, 24, 79). Consider the example of the Brownian motion of an inert colloid suspended in a solvent: during a given time interval τ, the MSD of the particle does indeed go as τ, except when the time interval is very small, for example, the interval between collisions. At these very small timescales, the particle may appear to be undergoing what is defined as ballistic motion as it traverses its mean free path between solvent collisions (96). For particles that migrate along a linear trajectory with a constant ballistic velocity, $\alpha = 2$. In contrast, however, labeled messenger RNA molecules in a living *Escherichia coli* cell undergo subdiffusion with α values of approximately 0.7 (79).

INSPIRATIONS FROM NATURE

A motor is a machine that consumes some form of energy and converts it into mechanical work. Motion is an inextricable part of life, and nature has employed several different chemically powered motors to sustain life. Some examples of molecular motors include myosins, dyneins, and kinesins, all of which are known as cytoplasmic motors. These molecules utilize ATP as their energy source and achieve directionality by moving on tracks (e.g., microtubules). ATP hydrolysis causes a conformational change that is further amplified and translated into mobility. In this respect, synthetic motors and pumps are similar to their biological counterparts. Both biological and synthetic motors expend energy: Biological motors utilize ATP hydrolysis and convert it into mechanical motion, and synthetic motors use chemical, electrical, or magnetic energy to do the same. The working mechanisms of these two kinds of motors often resemble each other: Specifically, proton gradients cause transport across membranes in living systems and

are responsible for the propulsion of bimetallic nanorods and fluid pumping in bimetallic pumps (see the subsection titled "Self-electrophoresis") (64). Although synthetic motors do exhibit directionality, another interesting goal involves motion along a predefined track, replicating kinesin translocation along a microtubule. A recent study reveals that almost all enzymes, not just the ones functioning as cytoplasmic motors, are capable of exhibiting motion. Further, these enzymes exhibit a rudimentary form of chemotaxis in the presence of their substrate gradient (see the subsection titled "Enzyme Motors and Pumps").

The following subsections discuss two classical biological molecular machines: the dynein motor that powers the motion of cilia and flagella (57, 100), and the classical sodium–potassium pump (17). Their synthetic analogs have also been constructed and are discussed in the sections titled "Synthetic Adaptations" and "Artificial Motors and Pumps for Biomedical Applications."

Cilia and Flagella

For individual cilia and flagella, the *Re* falls between 10^{-4} and 10^{-6}. For *Re* values in this range, the inertial force takes into account the mass and propulsion velocity of the organism, and the viscous forces are derived from the liquid environment of the organism.

Cilia and eukaryotic flagella enable organisms to exhibit motility. Both are driven by dynein motors and utilize ATP as a primary energy source, helping the organism move to new sources of food and, in turn, giving motile species a marked advantage over their nonmotile counterparts. The oscillations produced by cilia and eukaryotic flagella translate into an average forward motion (37). In prokaryotes, motility is exhibited by flagella that are anchored on the inner cell membrane and that undergo rotary motion powered by motors at their bases (7). The motor for each flagellum derives its power from a proton or sodium ion flux across the bacterial cell membrane.

Although some organisms propel themselves using single flagella, others can enjoy enhanced locomotion by phase adjusting the oscillatory beat patterns of individual flagella in their flagellar bundles (14, 45). Similar favorable interactions are also observed in groups of individual organisms moving in close proximity to each other. The subsection titled "Emergent Collective Behavior" discusses these phenomena and their laboratory counterparts in greater detail.

Cilia are tiny hair-like structures that are essentially short flagella that occur in large arrays, and neighboring cilia cause fluid flow by synchronous movement stemming from an in-phase relationship between their beats (9). The synchronized beating of neighboring cilia produces metachronal waves that in turn accomplish complex tasks including fluid motion and sensing. As an example, fluid motion induced by the cilia lining the gills of nonmotile marine animals is vital for water ingestion and filter feeding (116). These tiny antennas can be triggered by external mechanical or chemical stimuli. Stimulation of the cilia in turn initiates complex cascading chemical reactions that help transmit signals within the cells (29, 110). Cilia are also involved in sensing; for example, fish use hair-like sensors to detect fluid disturbances made by approaching predators (28). The importance of ciliary systems also extends to other areas: For example, cilia lining the brain ventricles have a significant effect on transmural transport (113). Similarly, a single California mussel, *Mytilus californianus*, can remove impurities suspended in water using its cilia-lined gills at an average filtration rate of 2.6 L/h (27).

Axonemes form the core structures of the eukaryotic cilia and flagella. Dynein motors are important building blocks of axonemes and provide the power for ciliary and flagellar motility. Dyneins form the basic framework of the nine cylindrically arranged microtubule (MT) doublets in each axoneme. The oscillatory beats produced by flagella and cilia result from an ATP-driven mechanochemical cycle, in which the dynein motor on one MT doublet interacts with the

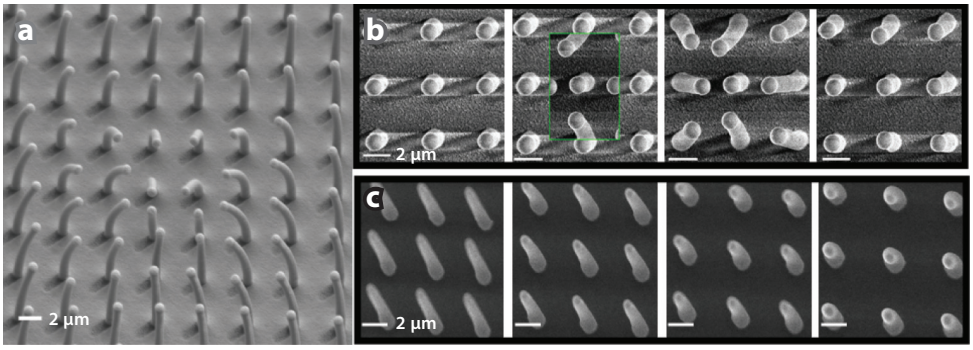

Figure 1

Scanning electron microscope image of synthetic ciliated surface. (*a*) The surface was fabricated using soft lithography and actuated using an electron-beam. (*b* and *c*) Actuated epoxy nanoposts are observed to reversibly bend and tilt within seconds of electron-beam focusing. Figure adapted from Reference 95 with permission from John Wiley and Sons.

binding sites on the adjoining doublet, resulting in sliding motion that is subsequently converted to bending (57, 100).

Because of the myriad of potential applications, current research efforts are focused on replicating the efficient natural motor systems (66, 95, 111, 112, 124, 125, 143) (**Figure 1**). Actuated synthetic cilia can be employed to alter the fluid environment locally and to regulate transport at surfaces. As observed in nature, controlling the shape, size, and oscillation frequency of the structural material enables a broad range of microfluidic applications. Lab-on-a-chip devices integrate several laboratory functions into a single small-scale chip, and these devices require regulated fluid transport that can be achieved by ciliated surfaces. Studies have also demonstrated that surfaces embedded with cilia-like nanostructures show self-cleaning and self-repair properties (95, 112, 135).

Although mimicking the independent actuation of individual biocilia presents a formidable challenge, one study has demonstrated coordinated movement using magnetic actuation (133). In addition, Dogic and coworkers (104) have replicated a ciliary beating pattern using a bottom-up approach. They used biotin labeled kinesin motors bound into clusters through streptavidin-stabilized microtubules. Polyethylene glycol was added to induce attractive interactions between the MTs. This design enables the kinesin clusters to simultaneously bind and walk along the neighboring MTs.

The in vitro artificial design described above enabled the study of both isolated active microtubule bundles and synchronous emergent behavior arising from interacting beating bundles, for example, metachronal waves observed in cilia. Importantly, however, it also provides a design for active materials for fluid transport. Finally, Aizenberg and colleagues developed surfaces bearing arrays of nanostructures put in motion by environment-responsive gels that can be designed to confer a wide range of adaptive motion-generating, self-cleaning and other behaviors (95, 112, 135).

The Sodium–Potassium Pump

The transport of ions and molecules into and out of cells is critical to the functioning of cellular machinery. Both transport against concentration gradients and movement of hydrophilic molecules across lipid bilayers pose challenges that are overcome by active transport. The movement of sodium and potassium against concentration gradients is effected by the Na^+/K^+ ATPase, a membrane-bound ion pump. The energy for this action is derived from ATP hydrolysis, which

the enzyme uses to generate electrochemical gradients for Na^+ and K^+ across the plasma membranes of cells (23, 114, 115). Such electrochemical gradients play a critical role in the cellular uptake of ions and nutrients and in the regulation of intracellular pH and cell volume. This ion transport is made possible by conformational changes in the Na^+/K^+ ATPase; the two conformational states of the ATPase selectively bind three Na^+ ions and two K^+ ions. Hence, for every hydrolyzed ATP molecule, three Na^+ ions are exported, and two K^+ ions are imported. Some functional aspects of these naturally occurring pumps have been duplicated in the laboratory (137), and the subsection titled "Diffusiophoretic Motors" discusses them in greater detail.

SYNTHETIC ADAPTATIONS

Researchers have designed several synthetic, self-powered micron-sized and nano-sized machines inspired by biological counterparts. To overcome the dominance of viscous forces and randomization from Brownian motion in low-*Re* regimes, asymmetric swimming and a constant net force are necessary to induce motion of either the machines themselves or the ambient fluid. In the following subsection, we discuss new advances in the design of synthetic motors and pumps and the recent discovery of enzymes as new molecular machines and pumps.

Synthetic Motors and Pumps

Motors and pumps are the two major synthetic machines of interest, and both generate mechanical forces and cause directional transport by converting energy either from chemical fuels (34, 39, 41, 48, 61, 87, 91, 92, 118, 121, 136, 140, 141) or from external sources including magnetic (20, 33, 36, 123), electric (11, 13), light (1, 47, 70, 86), acoustic (2, 54, 132), and thermal fields (6, 52, 97). Unlike motors that propel themselves, pumps do not move themselves; rather, they induce the movement of nearby fluids and inert tracer particles. The motors require a gradient along the surface (e.g., in chemical concentration, temperature, surface tension, or pressure) to induce motion. They are mostly designed as rods or spheres that have asymmetric compositions (e.g., Janus particles, which have an active material on one side and an inert material on the other) (39), activity (different chemical reaction rates at the two ends) (93), or shape (e.g., motors that are concave on one end and convex on the other) (129). Early micropump designs were based on the generation of local electric fields (47, 51, 62, 77, 90, 92). Recent designs include polymeric or enzymatic micropumps, which pump fluids by generating chemical concentration gradients (108, 109, 139, 142).

Propulsion Mechanisms

The generation of the propulsive force, asymmetry, and, ultimately, motion can arise from a variety of mechanisms. These mechanisms may be based on either chemical concentration gradients, as in self-electrophoresis and self-diffusiophoresis, or the gradients of external fields.

Self-electrophoresis. Electrophoresis is a phenomenon in which charged species are transported through a liquid medium (usually an aqueous solution) under an electric field. In an electric field (E), charged particles migrate with velocity ($\mathbf{U}$) governed by the Smoluchowski equation for particles with thin double layers (3, 117):

$$\mathbf{U} = \frac{\zeta_p \varepsilon}{\mu} E. \qquad 5.$$

Here, ζ_p is the zeta potential of the particle surface, which is related to the surface charge, and ε and μ are the permittivity and dynamic viscosity of the medium, respectively. Unlike conventional

electrophoresis, which requires an external electric field, redox reactions occurring at different parts of a particle surface can result in an ion concentration gradient, and hence local electric field, leading to the motion of the object itself. This process is called self-electrophoresis, and it has been exploited in various synthetic micromachine and nanomachine systems over the past decade.

The first such system was discovered by the Sen and Mallouk groups at The Pennsylvania State University (93). In this system, Au–Pt nanorods (2–3 μm long and ~400 nm in diameter) were observed to move autonomously in dilute hydrogen peroxide (H_2O_2), with the Pt ends leading at a speed of approximately 10 μm/s. The Ozin group (26) independently made similar observations with Au–Ni nanorods of similar dimensions.

In self-electrophoresis, the charged microparticle moves in a self-generated electric field as a result of an asymmetric distribution of ions. For example, **Figure 2*a*** shows that in the case of Au–Pt bimetallic nanomotors, oxidation of H_2O_2 occurs at the anode (Pt end), and reduction of H_2O_2 (and that of O_2) occurs at the cathode (Au end), leading to a proton concentration gradient oriented from the Pt end to the Au end. This asymmetric distribution results in an electric field that has the opposite direction as the proton concentration gradient. The negatively charged nanorod therefore moves toward the Pt end, an effect similar to traditional electrophoresis.

The discovery of bimetallic motors has inspired the design of other synthetic machines, including motors that are based on different shapes (38, 134), fuels (71, 75), and power sources (72). **Figure 2*b*** shows that redox chemical reactions that are responsible for self-electrophoresis and motor propulsion can also be triggered by electric fields by means of bipolar chemistry. In one such system, Zn micromotors are propelled under an electric potential: Zn metal is oxidized and dissolved at one end, and Zn ions are reduced, and metal deposited, at the other end.

Micropumps that are based on self-electrophoresis have also been designed. A motor moves through fluid, so by inverse, immobilizing it will induce fluid flow in the vicinity of the motor. The first examples of micropumps (51, 53, 60, 62, 63) were developed using the same principle as those used in the development of bimetallic Au–Pt motors (described above). When fuel is added to the system, electrochemical reactions take place at the surface of the two metals: The cathode reduces fuel and consumes protons, and the anode oxidizes fuel and produces protons (see **Figure 2*c***). The redox reaction creates a proton gradient in solution over the metals, and thus it also creates an electric field. This field acts both phoretically on charged tracer particles and osmotically on the electric double-layer on the charged metal surface, leading to fluid motion. Only the electrophoretic effect matters in determining the direction of motion for tracer particles suspended in solution, whereas the combination or competition of the electrophoretic and electroosmotic effects decides the direction of movement for particles near the metal surface. Changing the fuel can lead to changes in pumping direction, as demonstrated in **Figure 2*d***.

Self-diffusiophoresis. Similar to self-electrophoresis, self-diffusiophoresis is a mechanism that originates from chemical concentration gradients that are produced by surface chemical reactions. Self-diffusiophoresis can be classified into two categories, electrolyte and nonelectrolyte self-diffusiophoresis, depending on whether the chemical species contributing to the gradient are charged or uncharged, respectively.

Electrolyte self-diffusiophoresis. Electrolyte self-diffusiophoresis is more commonly exploited in the synthetic motor and pump systems. This mechanism works when a gradient of electrolytes ∇c is formed across a charged surface with zeta potential ζ_p. For diffusiophoresis near a wall with zeta potential ζ_w, two effects contribute to the movement of a particle: an electrophoretic effect

and a chemophoretic effect. In such cases, the speed U of the diffusiophoretic movement can be approximated by Equation 6 (3):

$$U = \underbrace{\frac{\nabla c}{c_0}\left[\left(\frac{D^+ - D^-}{D^+ + D^-}\right)\left(\frac{k_B T}{e}\right)\frac{\varepsilon(\zeta_p - \zeta_w)}{\eta}\right]}_{\text{Electrophoretic Term}} + \underbrace{\frac{\nabla c}{c_0}\left[\left(\frac{2\varepsilon k_B^2 T^2}{\eta e^2}\right)\left\{\ln\left(1-\gamma_w^2\right) - \ln\left(1-\gamma_p^2\right)\right\}\right]}_{\text{Chemophoretic Term}}, \quad 6.$$

where D^+ and D^- are the diffusion coefficients of the cation and anion, respectively, c_0 is the bulk concentration of ions, e is the charge of an electron, k_B is the Boltzmann constant, T is the

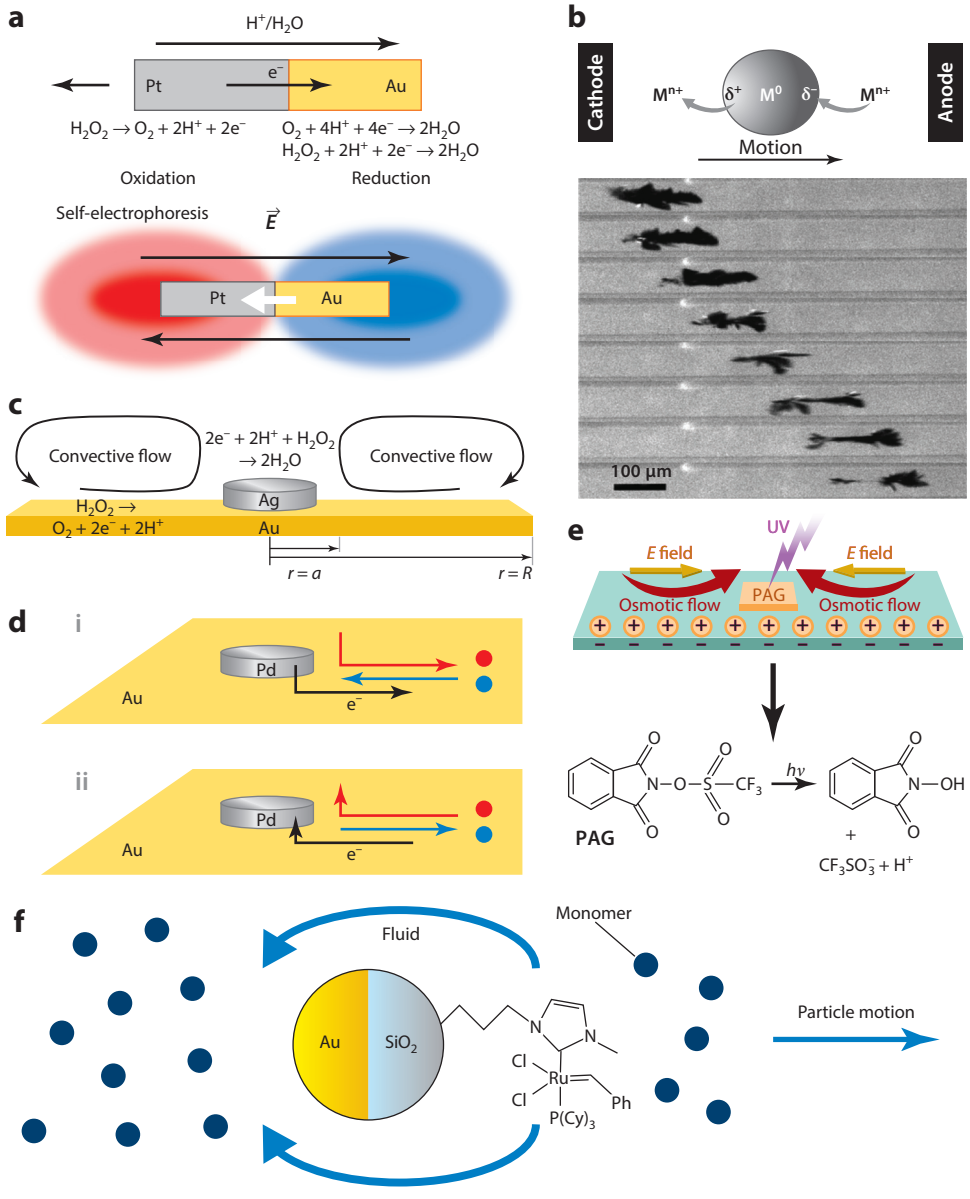

Figure 2

Micromotors and pumps with different propulsion mechanisms. (*a*) Propulsion of bimetallic Au–Pt nanorods in H_2O_2 solution powered by self-electrophoresis. Panel adapted from Reference 93, with permission from the American Chemical Society. (*b*) Propulsion of Zn microparticles in 0.1 M zinc sulfate solution mediated by bipolar chemistry under an external electric field. Panel adapted from Reference 72, with permission from the American Chemical Society. (*c*) Immobilization of bimetallic motors on a surface induces fluid flows in its vicinity. Panel adapted from Reference 62, with permission from the American Chemical Society. (*d*) Direction of movement of negative SiO_2 colloids (*blue*), positive amidine-functionalized colloids (*red*), and electrons (*black*) over an Au surface relative to a Pd feature in a solution containing different fuels: (*i*) hydrazine (N_2H_4) or (*ii*) dimethyl hydrazine ($N_2Me_2H_2$). Panel adapted from Reference 51, with permission from the American Chemical Society. (*e*) Exposure to ultraviolet (UV) light leads to formation of ions from the photoacid generator (PAG). The faster diffusivity of protons leads to inward electric fields that act both phoretically on the colloids and osmotically on the ions near the charged substrate surface. The combination of the two causes inward motion of positive, amine-functionalized polystyrene (NH_2-PS) particles, which gather around the photoacid. Panel adapted from Reference 139, with permission from the American Chemical Society. (*f*) Propulsion of a Janus particle under nonelectrolyte self-diffusiophoresis owing to ring-opening metathesis polymerization of norbornene (monomer) by the immobilized Ru catalyst. Panel adapted from Reference 91, with permission from John Wiley & Sons.

absolute temperature, ε is the dielectric permittivity of the solution, η is the viscosity, and $\gamma_w = \tanh(e\zeta_w/4k_BT)$, $\gamma_p = \tanh(e\zeta_p/4k_BT)$. If the cation and the anion exhibit different diffusivities, a net electric field emerges, resulting in the electrophoretic term in Equation 6. The electric field acts both diffusiophoretically on the nearby charged particles and osmophoretically on the fluid near the double layer of the wall. The interplay between phoretic and osmotic components depends on the difference between the zeta potentials of the particles (ζ_p) and the wall (ζ_w), and this interplay can lead to schooling and exclusion behaviors that are discussed later in the subsection titled "Self-assembly and collective patterns." In addition, because ionic strength influences the thickness of the electric double layer, the electrolyte concentration gradient causes a gradient in the thickness of the electric double layer. Higher "pressure" where the double layer is thinner drives fluid flow from an area of relatively high electrolyte concentration to one of lower concentration. This behavior is described by the chemophoretic term in Equation 6. In most cases, the chemophoretic effect is negligible, and diffusiophoretic transport is governed by the electrophoretic effect, unless the diffusivities of the cations and the anions are very similar.

Because of their high diffusivities and significant contribution to electrophoretic effect, self-diffusiophoretic systems often involve chemical reactions that generate gradients of H^+ or OH^-. The first example of such a system is the UV light–powered silver chloride (AgCl) micromotor reported by Ibele et al. (49). Under UV light, AgCl is reduced to Ag metal, and produces protons and chloride ions. Because protons have a significantly higher diffusivity ($D_{H^+} = 9.311 \times 10^{-5}$ cm^{2}s^{-1}, $D_{Cl^-} = 1.385 \times 10^{-5}$ cm^{2}s^{-1} at 298 K), an electric field is generated. This field points toward the AgCl particles and results in both electrophoresis of these particles and electroosmosis along the wall. Irregular shapes and/or different reactivities of the AgCl particles break the spherical symmetry around them, driving them into motion by means of the unbalanced electric field and diffusiophoretic flow. More recent electrolyte self-diffusiophoretic systems employ other reactions, such as dissociation of acids (98), but these newer systems follow essentially the same protocol. Such a protocol can also be extended to design micropumps that drive fluid motion via photogeneration of ions (139) (**Figure 2*e***) or dissolution of salts (138).

Nonelectrolyte self-diffusiophoresis. As shown in Equation 6, high electrolyte concentrations suppress electrolyte-driven diffusiophoretic transport, and, as a result, synthetic machines powered by

this mechanism cannot operate in media with high ionic strengths. Thus, although the propulsive forces generated by nonelectrolyte diffusiophoresis (based on neutral solute gradients) are generally weaker than those generated by its electrolyte analog, this mechanism remains effective in powering motion at high ionic strength. Pavlick et al. (91) described one such system: The catalysis of norbornene polymerization by a Grubbs catalyst attached to the SiO_2 end of a SiO_2–Au Janus particle resulted in the enhanced diffusivity of Janus spheres. The propulsive force in the system is believed to arise from the asymmetric distribution of monomer molecules on the two sides of the sphere, as monomers are consumed on the catalyst end (SiO_2 end) (see **Figure 2*f***). Consumption of the monomer by the Grubbs catalyst attached on the particle surface creates a monomer gradient that leads to a pressure gradient. This gradient in turn powers the motion of the particles (16, 40). The inverse of this polymerization-powered motor system, in which one side of the particle creates more solute molecules than the other, has also been explored (32, 48, 58, 142).

Self-electrophoresis versus electrolyte self-diffusiophoresis. Self-electrophoresis and electrolyte self-diffusiophoresis are two of the most commonly exploited mechanisms for the design of synthetic micromachines and nanomachines. Both mechanisms are based on surface chemical reactions and on the generation of chemical gradients and local electric fields. The differences between the two mechanisms and the associated systems can be summarized as follows. Electric fields generated by self-electrophoretic motors are more localized and do not extend as far as those generated by electrolyte self-diffusiophoretic systems. As a result, interactions between the self-electrophoretic motors are short range, leading to only the assembly of doublets or triplets, whereas electrolyte self-diffusiophoretic interactions can lead to the formation of collective patterns such as schools. In addition, interactions between self-electrophoretic motors are anisotropic and are highly influenced by the relative positions and/or orientations of the motors. Electrolyte self-diffusiophoretic motors, in contrast, can emit and receive chemical signals in an isotropic manner. Lastly, formation of electric fields requires self-electrophoretic systems to be conductive (67), which is not necessary for their electrolyte self-diffusiophoretic counterparts.

Other mechanisms. Bubble propulsion is another mechanism that can power motion at high ionic strengths. In this mechanism, oxygen or hydrogen microbubbles are generated via H_2O_2 decomposition or reduction of water. When bubbles detach from the motors, the associated recoil force pushes the motors in the opposite direction (35, 39, 83, 119).

Many other important propulsion mechanisms exist in addition to those discussed in the preceding subsections. These include mechanisms based on self-generated gradients, such as self-acoustophoresis and self-thermophoresis, as well as mechanisms that follow the gradients generated by external fields including, for example, electric and magnetic fields. We present specific examples of and elaborate further on these mechanisms in the subsection titled "Enzyme Motors and Pumps" and the section "Artificial Motors and Pumps for Biomedical Applications." A few review articles touch upon these topics and are recommended for interested readers (25, 42, 78, 84).

Emergent Collective Behavior

Communication and cooperation between individual agents are commonly observed in natural systems, and the subsequent self-organization of these agents can lead to the emergence of biological phenomena such as locust swarms, flocking birds, and ant colonies. The transition from individual to collective behavior arises from the interactions of units in response to the changes in their local environment. These emergent systems are inspirations for the design of micromachines or nanomachines that can communicate and cooperate with each other to achieve potential

applications in the fields of drug delivery, particle assembly, and chemical sensing (4, 18, 31, 44, 55, 56, 74, 85, 89, 103, 122, 127).

Chemotaxis. Micromotors and nanomotors that are powered by chemical gradients can move preferentially in a direction defined by an externally applied chemical gradient, a phenomenon known as chemotaxis. Chemotaxis has long been observed in biological systems (8), and it has also been observed recently in synthetic systems and in enzymes in vitro (5, 46, 91, 106), although the mechanism in the latter systems is not as well-understood. When Pt–Au nanorods are placed in a gradient of H_2O_2, they gradually diffuse to the source of the chemical, using a combination of active and stochastic diffusion (see **Figure 3*a***) (46). A similar behavior was also discovered in the polymerization motor system discussed in subsection titled "Nonelectrolyte self-diffusiophoresis" (91), as well as in bubble-propelled catalytic microengines (5). Hong et al. (46) have proposed that catalytic motors preferentially diffuse up fuel concentration gradients to regions with higher diffusivities, and a similar mechanism has recently been described by Saha et al. (101).

Self-assembly and collective patterns. Similar to many natural systems, synthetic micromotors and nanomotors respond to externally generated chemical gradients and interact to form assemblies or collective patterns. For example, self-propelling bimetallic nanomotors that are moving in the same directions can attract each other to form doublets or even triplets (131). In addition, many collective micromotor systems have been designed based on the electrolyte self-diffusiophoresis mechanism. For example, AgCl micromotors can interact with each other when the particle concentration is increased (105) and can cluster to form so-called schools that resemble the behavior of flocking birds and schooling fishes (49). A predator–prey behavior is observed when negatively charged passive SiO_2 particles are added to this system, as the SiO_2 particles also respond to ion gradients generated by the active AgCl particles (**Figure 3*b***). Micromotor systems that show interactions over long distances can be designed by incorporating other chemical reactions. For example, researchers have observed spatiotemporal oscillation patterns among AgCl and SiO_2 particles under UV light in H_2O_2 solution (50). In addition, coupling different reactions may result in transitions between two collective behavior patterns: Duan et al. (22) reported that silver orthophosphate microparticles (Ag_3PO_4) in aqueous media show transitions between "exclusion" and "schooling" behaviors, which are triggered either by shifts in the chemical equilibrium (via addition or removal of ammonia) or in response to UV light (**Figure 3*c***). Because each different combination of two inputs (ammonia and UV) results in one of two outputs (schooling and exclusion), one can design a NOR logic gate, opening up a new avenue for computations using synthetic nanomachines and micromachines.

Enzyme Motors and Pumps

Recent studies have shown that most active enzymes can harvest energy from substrate turnover to generate mechanical force. This force powers the movement of the enzymes themselves and that of nearby particles, as well as the pumping of the surrounding fluid.

Enzyme motors. It has been demonstrated that similar to other chemically driven motors, enzymes are able to power their own motion by turnover of their respective substrates (10, 106). This ability is manifested in the form of substrate-dependent enhancement in diffusivity, as measured at the single-molecule level using fluorescence correlation spectroscopy (FCS). The observed diffusion enhancement disappears upon the addition of an inhibitor. The precise mechanism for turnover-induced enhanced diffusivity remains to be established, although several mechanistic

possibilities have been suggested. In one proposal, enzymes in solution propel themselves during substrate turnover by undergoing a sequence of nonreciprocal conformational changes during the substrate-binding and product-release steps (102). Alternatively, Colberg & Kapral (15) have suggested that molecular-scale catalysts can propel themselves via the production of products that can interact with the catalyst via Lennard-Jones interaction potentials. Spatially asymmetric

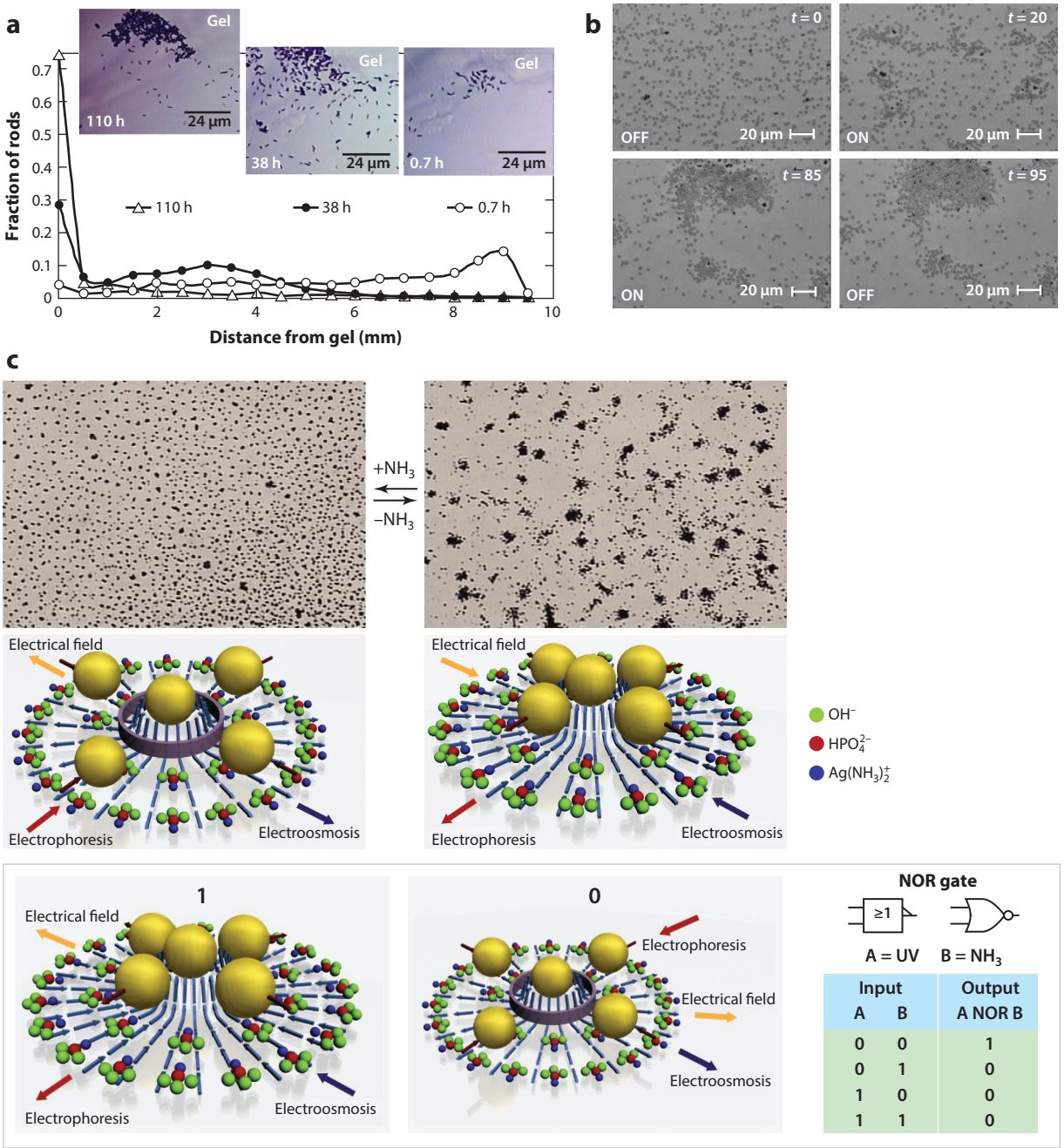

Input A	Input B	Output A NOR B
0	0	1
0	1	0
1	0	0
1	1	0

Figure 3

Collective behavior demonstrated by synthetic nanomotors and micromotors. (*a*) Chemotaxis of Au–Pt bimetallic nanomotors toward the source of H_2O_2 fuel (gel in the upper part of each image), depicted as an increase in the number of rods over time. Panel adapted from Reference 46, with permission from the American Physical Society. (*b*) Formation of predator–prey schools of active AgCl micromotors (*black dots*, prey) and inert SiO_2 tracer particles (*gray dots*, predators) under ultraviolet (UV) light. Panel adapted from Reference 49, with permission from John Wiley & Sons. (*c*) Reversible transition between two collective behaviors: Ag_3PO_4 micromotors disperse and cluster reversibly with the addition and removal of ammonia. The transition from dispersion to clustering can be halted by UV irradiation, and the two different responses of the micromotors under these two orthogonal inputs enable the design of a NOR logic gate. Panel adapted from Reference 22, with permission from the American Chemical Society.

catalysis can lead to an inhomogeneous distribution of products. This distribution creates a concentration gradient that can cause propulsion, depending on the features of the products and the solvent (self-diffusiophoresis). Finally, heat generation via reaction exothermicity can also lead to enhanced diffusion. In several instances, however, the bulk rise in solution temperature due to enzymatic catalysis has been estimated and found to be in the micro-Kelvin range; too small to account for the observed enhanced diffusion (106, 109). Nevertheless, a local, instantaneous, reaction-induced rise in temperature cannot be ruled out.

By using Langevin/Brownian dynamics simulations, it was determined that forces of 12 and 9 pN per turnover were sufficient to cause enhanced diffusion of urease and catalase, respectively. These forces are comparable to those produced by myosin, kinesin, and dynein motors (approximately 11 pN) (120) and by other molecular-scale systems (73, 77), and they are within the range needed to activate integrins (128), which are biological adhesion molecules responsible for mechanosensation by cells. Thus, force production by enzyme catalysis is a potentially novel and mechanobiology-relevant event.

In the presence of a gradient in substrate concentration, the enzyme molecules migrate toward regions with higher substrate concentrations—a form of molecular chemotaxis (106). It has been hypothesized (106, 109) that the chemotactic behavior of the enzyme molecules arises from the enhanced diffusion mechanism because the substrate concentration changes continuously as the enzyme diffuses along the gradient. Thus, at every point in space, the diffusion rate increases on moving up the gradient and decreases on moving down the gradient. A higher diffusion coefficient leads to greater spreading of the enzyme molecules in areas with high substrate concentrations, so the center of gravity of the enzyme ensemble moves toward higher substrate concentrations. As with any nonequilibrium system, continuous energy input is required for directional movement; in this case, energy input is needed to maintain the substrate gradient. The proposed mechanism is stochastic in nature and differs from biological chemotaxis, which requires temporal memory of the concentration gradient. The experimental findings on chemotaxis are supported by a finite-element simulation of the convection–diffusion equation in which the relationship between the enzyme diffusion coefficient and the substrate concentration was determined by FCS and was input into the simulation as a substrate concentration–dependent diffusion coefficient (106).

The observed chemotactic behavior of single enzymes suggests that when an enzyme acts on the products of a second enzymatic reaction nearby, the acting enzyme molecules might exhibit collective movement up the substrate gradient toward this second enzyme. This is an example of collective behavior at the molecular level. For example, catalase was observed to migrate toward glucose oxidase in the presence of glucose because H_2O_2 is a product in glucose oxidation (106).

The chemotactic migration of active enzymes toward areas of higher substrate concentration was utilized to separate enzymes from one another in a microfluidic device (19, 106). If one places a mixture of two enzymes in one channel and places the substrate for only one of them in the other

channel, the catalytically active biomolecules can be isolated from the corresponding inactive (or less active) ones. The procedure allows enzyme molecules of similar sizes and isoelectric points to be separated, and such separation is unprecedented in the literature. In principle, chemotactic separation can also be used to separate other active catalysts from their less-active or inactive counterparts in the presence of their respective substrates, so this technique should find wide applicability.

Enzyme pumps. Surface-anchored enzymes transfer their chemically generated force to the surrounding fluid; in effect, immobilized enzyme systems can be used as micropumps in the presence of enzyme-specific substrates (108). Thus, enzymes transduce chemical energy from substrate turnover into fluid motion. This discovery enables the design of nonmechanical self-powered enzyme-based devices that act as both sensor and pump, precisely controlling the flow rate and turning on and off in response to specific analytes. Most enzyme pumps that have been studied so far (glucose oxidase, catalase, lipase, DNA polymerase) catalyze exothermic reactions and therefore pump fluid and tracer particles inward along the bottom surface of a microchannel using thermal gradients (**Figure 4**). Urease (which hydrolyzes urea to bicarbonate and ammonium ions) increases the solution density, however, and thus pumps fluid outward. These experiments establish two important concepts: (*a*) Essentially all surface-anchored enzymes act as pumps during substrate turnover, and (*b*) these pumps are selective for the substrate or promoter of the particular enzyme.

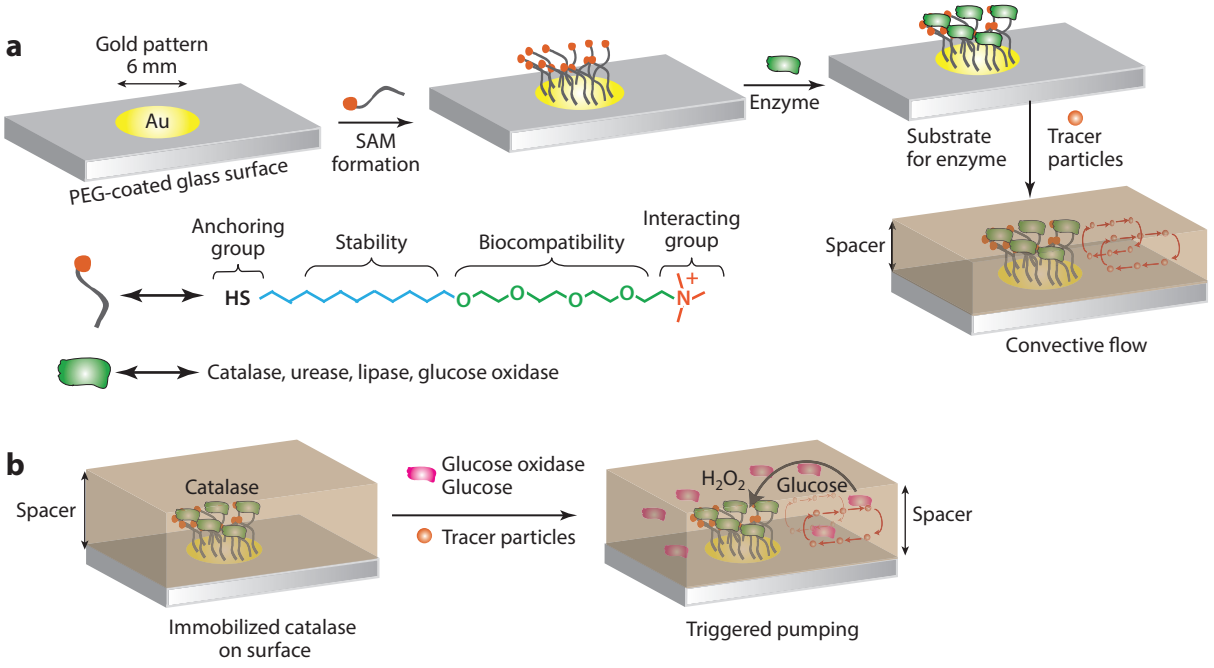

Figure 4

Schematic depiction of the fabrication and functioning of enzymatic micropumps. (*a*) Au patterned on a polyethylene glycol (PEG)-coated glass surface is functionalized with a quaternary ammonium thiol, which electrostatically binds to the negatively charged groups on the enzyme. Triggered fluid pumping is initiated by introducing the enzyme-specific substrate. (*b*) Cascading fluid pumping is observed when the enzyme catalase is actuated by production of its substrate in situ by the enzyme glucose oxidase and its substrate glucose, enabling microfluidic regulation and logic. Abbreviations: HS, thiol; SAM, self-assembled monolayer.

Like the diffusivity of freely swimming enzymes, the pumping velocity of the enzyme pumps increases with increasing substrate concentration and reaction rate. Similar pumping can also occur in gel particles in which the enzymes are immobilized. For example, bound glucose oxidase pumps insulin out of gel particles when glucose is added to the surrounding solution (108).

ARTIFICIAL MOTORS AND PUMPS FOR BIOMEDICAL APPLICATIONS

Inspired by biological counterparts discussed in the section titled "Inspirations from Nature," several artificial motors have been designed for potential biomedical applications, both in vivo and in vitro. These motors can be classified into four groups on the basis of how they are powered: diffusiophoretic motors, bubble-propelled motors, magnetically driven motors, or acoustically powered motors.

Diffusiophoretic Motors

Autonomous pumps based on ion gradients have been described previously and are of particular interest for orthopedic applications because of the high mineral content of bone. Yadav et al. (137) have reported a micropump-based strategy that utilizes the substrate itself as both the trigger and the fuel. Because this technique does not require an external power supply, it appears to be ideal for targeted drug delivery. Bone is composed of the mineral hydroxyapatite, which undergoes hydrolysis at physiological pH, as described by Equation 7.

$$Ca_{10}(PO_4)_6(OH)_2 + 12H_2O \rightarrow 10Ca^{2+} + 6H_2PO_4^- + 14OH^- \qquad 7.$$

A crack in a bone releases ions into the surrounding solution, and the large difference in diffusion coefficients between the cation (Ca^{2+}) and the faster anion (OH^-) [$D(Ca^{2+}) = 0.789 \times 10^{-5}$ cm^2/s, $D(OH^-) = 5.273 \times 10^{-5}$ cm^2/s, and $D(H_2PO_4^-) = 0.959 \times 10^{-5}$ cm^2/s] induces a local electric field pointed away from the crack in the bone surface (i.e., the ion source). Negatively charged moieties introduced into the system respond to this electric field by undergoing diffusiophoretic transport toward the damage site. Thus, the damaged matrix itself provides both the fuel and the trigger for detection and repair. **Figure 5*a*** shows how negatively charged quantum dots were used to demonstrate the detection process. In addition, the delivery of a bone growth factor incorporated into a polymeric particle was achieved. This technique provides a mechanism for actively targeting the damage site, in contrast to the traditional mechanism of transporting drugs via passive diffusion.

Bubble-Propelled Motors

Identification, separation, and isolation of target analytes, such as specific proteins, nucleic acids, or other biomarkers, are extremely important in biomedical research. Bubble-propelled motors can sense, capture, and transport biological analytes ranging from molecules to cells via surface modification and functionalization (119). In several publications, Wang and coworkers demonstrated that receptor-modified tubular microengines can selectively isolate a wide range of target bioanalytes, including bacteria (12), DNA molecules (136), and cancer cells (4). For example, catalytic microengines that have an outer surface functionalized with the Concanavalin A (ConA) lectin receptor can recognize and selectively bind to carbohydrate constituents of bacterial surfaces (12). As proof of this concept, these researchers demonstrated that *E. coli* can be isolated from untreated seawater and drinking water samples (**Figure 5*b***). With the help of external magnetic

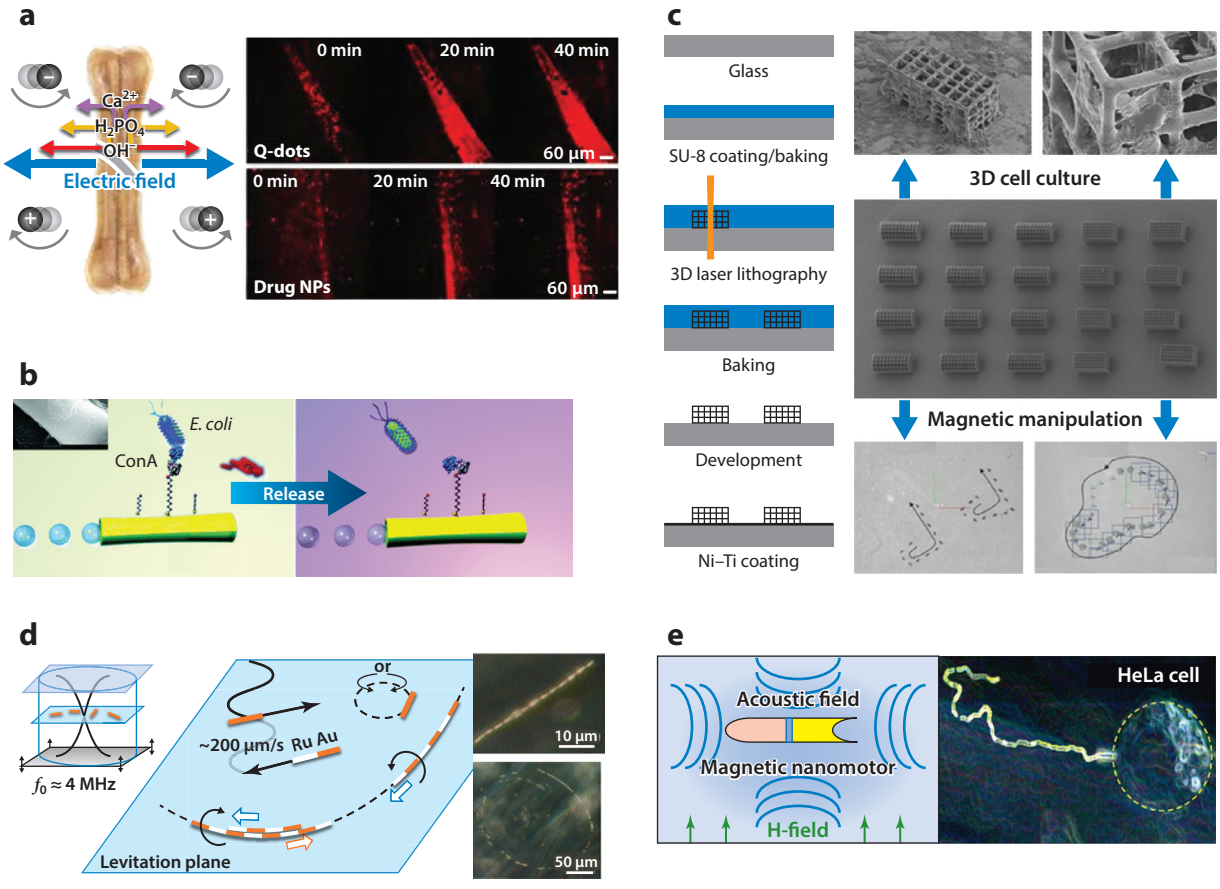

Figure 5

Artificial motors and pumps for biomedical applications. (*a*) Ions that leach from the bone crack induce self-diffusiophoretic flows that lead to the enrichment of negatively charged fluorescent quantum dots (Q-dots) and drug nanoparticles (NPs) at the crack site. Panel adapted from Reference 137, with permission from John Wiley & Sons. (*b*) Isolation of bacteria from seawater or drinking water samples using Concanavalin A (ConA) functionalized catalytic motors. Panel adapted from Reference 12, with permission from the American Chemical Society. (*c*) Fabrication and magnetic manipulation of cage-like micromotors for transportation of cells. Panel adapted from Reference 59, with permission from John Wiley & Sons. (*d*) Propagation and assembly of bimetallic rods under acoustic fields. Panel adapted from Reference 129, with permission from the American Chemical Society. (*e*) Navigation of an acoustically powered motor toward a HeLa cell under magnetic field guidance. Panel adapted from Reference 132, with permission from John Wiley and Sons. Abbreviations: *E. coli*, *Escherichia coli*.

fields, tubular catalytic microengines can function as concentrating systems (99) and can achieve directional transport and delivery of cells (103).

Bubble-propelled motors can be used to achieve controlled drug release by coating their surfaces with polymeric layers. For example, Mou et al. (82) demonstrated that Mg–Pt Janus motors coated with a thermoresponsive poly(N-isopropylacrylamide) (PNIPAM) hydrogel layer released drug molecules in response to a temperature change. Despite these potential applications, in vivo applications of bubble-propelled motors are hindered by electrolyte- and blood plasma–induced attenuation of their motility, as Pumera and colleagues reported (126, 144).

Magnetically Driven Motors

A problem for bubble-propelled motors is their general lack of directionality, owing to Brownian randomization at longer timescales. One way to overcome this problem is to introduce magnetic components into the motors. Although such motors are still powered by chemical fuels, they are also subject to guidance by external magnetic fields.

Another method is to simply replace the power source with external magnetic fields. Motors powered by external magnetic fields, when actuated, can be employed both in vitro and in vivo (94). Nelson and colleagues (30, 59, 81) reported several examples of cell transportation and drug delivery by artificial flagella using this technique. Cell transportation was accomplished by fabricating cage-like micromotors and allowing cells to grow inside them (see **Figure 5*c***). These motors were subsequently activated and propelled using an external rotating magnetic field (59). Drug delivery was accomplished using motor surfaces that were modified with drug-loaded chitosan or with liposomes (30, 81); these motors then migrated toward targets and released drugs.

Nelson and colleagues also reported wireless manipulation of micromotors inside eye cavity via the OctoMag electromagnetic control system (65, 76). The OctoMag can control motors in three dimensions, and it has a workspace of $\sim 20 \times 20 \times 20$ mm that covers the posterior segment of a human eye. Micromotors are injected into eyes using a 23G needle syringe, and, once inside, they are powered and manipulated with magnetic fields.

Acoustically Powered Motors

Low-power acoustic waves are safe and used extensively for in vivo imaging; thus, these waves are useful for powering motors. In an acoustic field, suspended microparticles experience acoustic radiation forces, which are strongest when standing waves are formed under acoustic excitation.

A recent work by Wang et al. (130) described a MHz-frequency ultrasound-powered autonomous micromotor system. In their system, bimetallic microrods are suspended in water and levitated to a plane at the midpoint of the cell by a vertical standing wave (**Figure 5*d***). In the plane, the rods exhibit axial propulsion at speeds as high as 200 μm/s (~100 body lengths per second). These bimetallic rods also form patterns in the nodal plane. Motion of the motors is significantly affected by their composition, as only metallic rods show fast axial motion; polymeric rods do not.

The exact propulsion mechanism is not completely understood, but self-acoustophoresis has been suggested as a possibility. Acoustic motors, under the guidance of magnetic fields, can be steered to capture and transport various bioanalytes, such as cells (**Figure 5*e***) (2). Wang and colleagues (132) also reported the motion of acoustic motors inside living HeLa cells. This report is the first example of artificial motors inside living cells. The motors attach strongly to the external surfaces of the cells, and they are readily internalized after incubation for periods of at least 24 h. These motors are actuated at 4 MHz, and they exhibit axial propulsion and spinning while the cells remain viable. Such systems can provide a new tool for probing the response of living cells to internal mechanical excitation and for related biomedical applications.

CONCLUSION

Challenges to the large-scale use of synthetic motors in biological systems include developing effective fabrication and optimal actuation mechanisms, precise control over motion, and biocompatibility. Synthetic motors, which are discussed in this review, can be divided roughly into two groups: motors that are powered externally by, for example, electric, magnetic, or acoustic fields, and motors that are powered by self-generated gradients, for example, those powered by self-electrophoresis and self-diffusiophoresis. In the former group, the external field is applied from a macroscopic source, and all of the motors are subject to similar forces and migrate along

the projected field lines. Such external control is a desired functionality for directed navigation. In comparison, motors that are powered by self-generated gradients are autonomous, in that each motor makes its own decision on the basis of its local environment. This ability to respond to an environment and to move autonomously grants versatility, and it is the foundation of collective behaviors such as swarming and schooling, which indicate intermotor communication. In addition it is beneficial to have motors that can independently carry out operations such as sensing and reporting, where different populations of interacting motors perform different tasks. Because the two kinds of motors have their own advantages, combining both propulsion methods in one single motor system would be desirable. Such a system would include motors that are orthogonally powered by external fields and self-generated gradients: The former can guide the directed migration to desired sites, and the latter enable communication and cooperation between motors.

Despite the reported progress in the design of synthetic motors, they cannot carry out complex tasks in the same manner as their biological counterparts. More integrated functionalities (69) and better division of labor are two key elements future designs of synthetic motors should consider. The ultimate goal in the emerging area of synthetic motors and pumps is to create functional building blocks that have the following attributes: (*a*) mobility resulting from biomimetic energy harvested from the local environment, (*b*) rapid and reversible assembly capabilities provided by emergent self-assembly, (*c*) the intelligence and communication capabilities seen in interacting microorganisms, and (*d*) the ability to perform specific tasks in response to signals from each other and from the environment.

The observation that enzymes such as urease, catalase, lipase, DNA polymerase, and others undergo powered movement and pump fluids while catalyzing substrate turnover amends the paradigm that ATP-powered biomotors are a special class of enzymes. This observation clearly suggests that (*a*) single-enzyme molecules generate sufficient mechanical force via substrate turnover to cause their own movement and that of the surrounding particles and fluid, and (*b*) the movement becomes directional when a gradient in substrate concentration is imposed. Indeed, other than the presence of so-called tracks that provide directionality, there may not be a significant difference between traditional motor proteins and free-swimming enzymes. In addition, it will be interesting to examine the role played by membrane-bound enzymes in cell membrane fluctuations. The results described open up a new area of mechanobiology: intrinsic force generation by non-ATP-dependent enzymes and their role in the biochemical regulation of cell function. These enzymes, as well as nontraditional ATP-dependent enzymes, can provide sufficient force for the stochastic motion of the cytoplasm and for the convective transport of fluid in cells (43). Further, they may be responsible for the observed glass-to-fluid transition that occurs in active bacterial cells (88).

SUMMARY POINTS

1. Nature displays efficient forms of biological motors and pumps that serve as inspirations for the design of both self-powered synthetic nanomotors and micromotors and pumps.
2. As the size of an object scales down, surface forces such as viscosity dominate over volume forces such as inertia. This shift in force dominance is characteristic of the low-*Re* regime.
3. Synthetic motors and pumps are powered by various propulsion mechanisms, such as electrophoresis, electrolyte and nonelectrolyte diffusiophoresis, and acoustophoresis.
4. Similar to many natural systems, the synthetic micromotors and nanomotors respond to chemical gradients generated by each other to form assemblies or collective patterns.

5. Non-ATP-powered enzymes generate sufficient mechanical force via substrate turnover to cause their own movement and that of the surrounding particles and fluid. The movement becomes directional through the imposition of a substrate gradient.
6. Surface-anchored enzymes transfer their chemically generated force to the surrounding fluid, in effect functioning as micropumps in the presence of their respective substrates.
7. Self-powered nanomotors and micromotors have many potential applications including the capture, transport, and concentration of bioanalytes, as well as the targeted delivery of drugs and antidotes in response to the presence of specific biomarkers.

DISCLOSURE STATEMENT

The authors are not aware of any affiliations, memberships, funding, or financial holdings that might be perceived as affecting the objectivity of this review.

ACKNOWLEDGMENTS

We gratefully acknowledge financial support from The Pennsylvania State University Materials Research Science and Engineering Center under National Science Foundation grant DMR-1420620 and supported in part by the Defense Threat Reduction Agency (HDTRA1-13-1-0039).

LITERATURE CITED

1. Abid J-P, Frigoli M, Pansu R, Szeftel J, Zyss J, et al. 2011. Light-driven directed motion of azobenzene-coated polymer nanoparticles in an aqueous medium. *Langmuir* 27:7967–71
2. Ahmed S, Wang W, Mair LO, Fraleigh RD, Li S, et al. 2013. Steering acoustically propelled nanowire motors toward cells in a biologically compatible environment using magnetic fields. *Langmuir* 29:16113–18
3. Anderson JL. 1989. Colloid transport by interfacial forces. *Annu. Rev. Fluid Mech.* 21:61–99
4. Balasubramanian S, Kagan D, Jack Hu C-M, Campuzano S, Lobo-Castañon MJ, et al. 2011. Micromachine-enabled capture and isolation of cancer cells in complex media. *Angew. Chem. Int. Ed.* 50:4161–64
5. Baraban L, Harazim SM, Sanchez S, Schmidt OG. 2013. Chemotactic behavior of catalytic motors in microfluidic channels. *Angew. Chem. Int. Ed.* 52:5552–56
6. Baraban L, Streubel R, Makarov D, Han L, Karnaushenko D, et al. 2012. Fuel-free locomotion of Janus motors: magnetically induced thermophoresis. *ACS Nano* 7:1360–67
7. Baykov AA, Malinen AM, Luoto HH, Lahti R. 2013. Pyrophosphate-fueled Na^+ and H^+ transport in prokaryotes. *Microbiol. Mol. Biol. Rev.* 77:267–76
8. Berg HC, Brown DA. 1972. Chemotaxis in *Escherichia coli* analysed by three-dimensional tracking. *Nature* 239:500–4
9. Brennen C, Winet H. 1977. Fluid mechanics of propulsion by cilia and flagella. *Annu. Rev. Fluid Mech.* 9:339–98
10. Butler PJ, Dey KK, Sen A. 2015. Impulsive enzymes: a new force in mechanobiology. *Cell. Molec. Bioeng.* 8:106–18
11. Calvo-Marzal P, Sattayasamitsathit S, Balasubramanian S, Windmiller JR, Dao C, Wang J. 2010. Propulsion of nanowire diodes. *Chem. Commun.* 46:1623–24
12. Campuzano S, Orozco J, Kagan D, Guix M, Gao W, et al. 2011. Bacterial isolation by lectin-modified microengines. *Nano Lett.* 12:396–401

13. Chang ST, Paunov VN, Petsev DN, Velev OD. 2007. Remotely powered self-propelling particles and micropumps based on miniature diodes. *Nat. Mater.* 6:235–40
14. Cleveland LR, Cleveland BT. 1966. The locomotory waves of *Koruga*, *Deltotrichonympha* and *Mixotricha*. *Arch. Protistenk* 109:39–63
15. Colberg PH, Kapral R. 2014. Angström-scale chemically powered motors. *Europhys. Lett.* 106:30004
16. Córdova-Figueroa UM, Brady JF. 2008. Osmotic propulsion: the osmotic motor. *Phys. Rev. Lett.* 100:158303
17. Dean RB. 1941. Theories of electrolyte equilibrium in muscle. *Biol. Symp.* 3:331–48
18. Detrain C, Deneubourg J-L. 2006. Self-organized structures in a superorganism: Do ants "behave" like molecules? *Phys. Life Rev.* 3:162–87
19. Dey KK, Das S, Poyton MF, Sengupta S, Butler PJ, et al. 2014. Chemotactic separation of enzymes. *ACS Nano* 8:11941–49
20. Dreyfus R, Baudry J, Roper ML, Fermigier M, Stone HA, Bibette J. 2005. Microscopic artificial swimmers. *Nature* 437:862–65
21. Duan W, Ibele M, Liu R, Sen A. 2012. Motion analysis of light-powered autonomous silver chloride nanomotors. *Eur. Phys. J. E* 35:77–84
22. Duan W, Liu R, Sen A. 2013. Transition between collective behaviors of micromotors in response to different stimuli. *J. Am. Chem. Soc.* 135:1280–83
23. Dubyak GR. 2004. Ion homeostasis, channels, and transporters: an update on cellular mechanisms. *Adv. Physiol. Educ.* 28:143–54
24. Dunderdale G, Ebbens S, Fairclough P, Howse J. 2012. Importance of particle tracking and calculating the mean-squared displacement in distinguishing nanopropulsion from other processes. *Langmuir* 28:10997–1006
25. Fischer P, Ghosh A. 2011. Magnetically actuated propulsion at low Reynolds numbers: towards nanoscale control. *Nanoscale* 3:557–63
26. Fournier-Bidoz S, Arsenault AC, Manners I, Ozin GA. 2005. Synthetic self-propelled nanorotors. *Chem. Commun.* 41:441–43
27. Fox DL, Coe WR. 1943. Biology of the California sea-mussel (*Mytilus californianus*). II. Nutrition, metabolism, growth and calcium deposition. *J. Exp. Zool.* 93:205–49
28. Fraser PJ, Shelmerdine RL. 2002. Dogfish hair cells sense hydrostatic pressure. *Nature* 415:495–96
29. Fratzl P, Barth FG. 2009. Biomaterial systems for mechanosensing and actuation. *Nature* 462:442–48
30. Fusco S, Chatzipirpiridis G, Sivaraman KM, Ergeneman O, Nelson BJ, Pané S. 2013. Chitosan electrodeposition for microrobotic drug delivery. *Adv. Healthcare Mater.* 2:1037–44
31. Gangwal S, Pawar A, Kretzschmar I, Velev OD. 2010. Programmed assembly of metallodielectric patchy particles in external AC electric fields. *Soft Matter* 6:1413–18
32. Gao W, Pei A, Dong R, Wang J. 2014. Catalytic iridium-based Janus micromotors powered by ultralow levels of chemical fuels. *J. Am. Chem. Soc.* 136:2276–79
33. Gao W, Sattayasamitsathit S, Manesh KM, Weihs D, Wang J. 2010. Magnetically powered flexible metal nanowire motors. *J. Am. Chem. Soc.* 132:14403–5
34. Gao W, Sattayasamitsathit S, Orozco J, Wang J. 2011. Highly efficient catalytic microengines: template electrosynthesis of polyaniline/platinum microtubes. *J. Am. Chem. Soc.* 133:11862–64
35. Garcia-Gradilla V, Orozco J, Sattayasamitsathit S, Soto F, Kuralay F, et al. 2013. Functionalized ultrasound-propelled magnetically guided nanomotors: toward practical biomedical applications. *ACS Nano* 7:9232–40
36. Ghosh A, Fischer P. 2009. Controlled propulsion of artificial magnetic nanostructured propellers. *Nano Lett.* 9:2243–45
37. Gibbons IR. 1981. Cilia and flagella of eukaryotes. *J. Cell Biol.* 91:107–24
38. Gibbs JG, Fragnito NA, Zhao Y. 2010. Asymmetric Pt/Au coated catalytic micromotors fabricated by dynamic shadowing growth. *Appl. Phys. Lett.* 97:253107
39. Gibbs JG, Zhao Y-P. 2009. Autonomously motile catalytic nanomotors by bubble propulsion. *Appl. Phys. Lett.* 94:163104
40. Golestanian R. 2009. Anomalous diffusion of symmetric and asymmetric active colloids. *Phys. Rev. Lett.* 102:188305

41. Golestanian R, Liverpool TB, Ajdari A. 2005. Propulsion of a molecular machine by asymmetric distribution of reaction products. *Phys. Rev. Lett.* 94:220801
42. Guix M, Mayorga-Martinez CC, Merkoçi A. 2014. Nano/micromotors in (bio)chemical science applications. *Chem. Rev.* 114:6285–322
43. Guo M, Ehrlicher AJ, Jensen MH, Renz M, Moore JR, et al. 2014. Probing the stochastic, motor-driven properties of the cytoplasm using force spectrum microscopy. *Cell* 158:822–32
44. Gupta S, Alargova RG, Kilpatrick PK, Velev OD. 2009. On-chip dielectrophoretic coassembly of live cells and particles into responsive biomaterials. *Langmuir* 26:3441–52
45. Hand WG, Haupt W. 1971. Flagellar activity of the colony members of *Volvox aureus* Ehrbg. during light stimulation. *J. Protozool.* 18:361–64
46. Hong Y, Blackman NMK, Kopp ND, Sen A, Velegol D. 2007. Chemotaxis of nonbiological colloidal rods. *Phys. Rev. Lett.* 99:178103
47. Hong Y, Diaz M, Córdova-Figueroa UM, Sen A. 2010. Light-driven titanium-dioxide-based reversible microfireworks and micromotor/micropump systems. *Adv. Funct. Mater.* 20:1568–76
48. Howse JR, Jones RAL, Ryan AJ, Gough T, Vafabakhsh R, Golestanian R. 2007. Self-motile colloidal particles: from directed propulsion to random walk. *Phys. Rev. Lett.* 99:048102
49. Ibele M, Mallouk TE, Sen A. 2009. Schooling behavior of light-powered autonomous micromotors in water. *Angew. Chem. Int. Ed.* 48:3308–12
50. Ibele ME, Lammert PE, Crespi VH, Sen A. 2010. Emergent, collective oscillations of self-mobile particles and patterned surfaces under redox conditions. *ACS Nano* 4:4845–51
51. Ibele ME, Wang Y, Kline TR, Mallouk TE, Sen A. 2007. Hydrazine fuels for bimetallic catalytic microfluidic pumping. *J. Am. Chem. Soc.* 129:7762–63
52. Jiang HR, Yoshinaga N, Sano M. 2010. Active motion of a Janus particle by self-thermophoresis in a defocused laser beam. *Phys. Rev. Lett.* 105:268302
53. Jun I-K, Hess H. 2010. A biomimetic, self-pumping membrane. *Adv. Mater.* 22:4823–25
54. Kagan D, Benchimol MJ, Claussen JC, Chuluun-Erdene E, Esener S, Wang J. 2012. Acoustic droplet vaporization and propulsion of perfluorocarbon-loaded microbullets for targeted tissue penetration and deformation. *Angew. Chem. Int. Ed.* 51:7519–22
55. Kagan D, Campuzano S, Balasubramanian S, Kuralay F, Flechsig G-U, Wang J. 2011. Functionalized micromachines for selective and rapid isolation of nucleic acid targets from complex samples. *Nano Lett.* 11:2083–87
56. Kagan D, Laocharoensuk R, Zimmerman M, Clawson C, Balasubramanian S, et al. 2010. Rapid delivery of drug carriers propelled and navigated by catalytic nanoshuttles. *Small* 6:2741–47
57. Kardon JR, Vale RD. 2009. Regulators of the cytoplasmic dynein motor. *Nat. Rev. Mol. Cell Biol.* 10:854–65
58. Ke H, Ye S, Carroll RL, Showalter K. 2010. Motion analysis of self-propelled Pt–Silica particles in hydrogen peroxide solutions. *J. Phys. Chem. A* 114:5462–67
59. Kim S, Qiu F, Kim S, Ghanbari A, Moon C, et al. 2013. Fabrication and characterization of magnetic microrobots for three-dimensional cell culture and targeted transportation. *Adv. Mater.* 25:5863–68
60. Kline TR, Iwata J, Lammert PE, Mallouk TE, Sen A, Velegol D. 2006. Catalytically driven colloidal patterning and transport. *J. Phys. Chem. B* 110:24513–21
61. Kline TR, Paxton WF, Mallouk TE, Sen A. 2005. Catalytic nanomotors: remote-controlled autonomous movement of striped metallic nanorods. *Angew. Chem.* 117:754–56
62. Kline TR, Paxton WF, Wang Y, Velegol D, Mallouk TE, Sen A. 2005. Catalytic micropumps: microscopic convective fluid flow and pattern formation. *J. Am. Chem. Soc.* 127:17150–51
63. Kline TR, Sen A. 2006. Reversible pattern formation through photolysis. *Langmuir* 22:7124–27
64. Kocherginsky N. 2009. Acidic lipids, H^+-ATPases, and mechanism of oxidative phosphorylation. Physico-chemical ideas 30 years after P. Mitchell's Nobel Prize award. *Prog. Biophys. Mol. Biol.* 99:20–41
65. Kummer MP, Abbott JJ, Kratochvil BE, Borer R, Sengul A, Nelson BJ. 2010. OctoMag: an electromagnetic system for 5-DOF wireless micromanipulation. *IEEE Trans. Robot.* 26:1006–17
66. Kwak MK, Jeong H-E, Kim T-I, Yoon H, Suh KY. 2010. Bio-inspired slanted polymer nanohairs for anisotropic wetting and directional dry adhesion. *Soft Matter* 6:1849–57

67. Laocharoensuk R, Burdick J, Wang J. 2008. Carbon-nanotube-induced acceleration of catalytic nanomotors. *ACS Nano* 2:1069–75
68. Lauga E. 2011. Enhanced diffusion by reciprocal swimming. *Phys. Rev. Lett.* 106:178101
69. Liu M, Liu L, Gao W, Su M, Ge Y, et al. 2014. A micromotor based on polymer single crystals and nanoparticles: toward functional versatility. *Nanoscale* 6:8601–5
70. Liu M, Zentgraf T, Liu Y, Bartal G, Zhang X. 2010. Light-driven nanoscale plasmonic motors. *Nat. Nanotechnol.* 5:570–73
71. Liu R, Sen A. 2011. Autonomous nanomotor based on copper–platinum segmented nanobattery. *J. Am. Chem. Soc.* 133:20064–67
72. Loget G, Kuhn A. 2010. Propulsion of microobjects by dynamic bipolar self-regeneration. *J. Am. Chem. Soc.* 132:15918–19
73. Mahadevan L, Matsudaira P. 2000. Motility powered by supramolecular springs and ratchets. *Science* 288:95–100
74. Manesh KM, Balasubramanian S, Wang J. 2010. Nanomotor-based 'writing' of surface microstructures. *Chem. Commun.* 46:5704–6
75. Mano N, Heller A. 2005. Bioelectrochemical propulsion. *J. Am. Chem. Soc.* 127:11574–75
76. Marino H, Bergeles C, Nelson BJ. 2014. Robust electromagnetic control of microrobots under force and localization uncertainties. *IEEE Trans. Automat. Sci. Eng.* 11:310–16
77. Mehta AD, Rief M, Spudich JA, Smith DA, Simmons RM. 1999. Single-molecule biomechanics with optical methods. *Science* 283:1689–95
78. Mei Y, Solovev AA, Sanchez S, Schmidt OG. 2011. Rolled-up nanotech on polymers: from basic perception to self-propelled catalytic microengines. *Chem. Soc. Rev.* 40:2109–19
79. Metzler R, Jeon J-H, Cherstvy AG, Barkai E. 2014. Anomalous diffusion models and their properties: non-stationarity, non-ergodicity, and ageing at the centenary of single particle tracking. *Phys. Chem. Chem. Phys.* 16:24128–64
80. Metzler R, Klafter J. 2000. The random walk's guide to anomalous diffusion: a fractional dynamics approach. *Phys. Rep.* 339:1–77
81. Mhanna R, Qiu F, Zhang L, Ding Y, Sugihara K, et al. 2014. Artificial bacterial flagella for remote-controlled targeted single-cell drug delivery. *Small* 10:1953–57
82. Mou F, Chen C, Zhong Q, Yin Y, Ma H-R, Guan J. 2014. Autonomous motion and temperature-controlled drug delivery of Mg/Pt-poly(N-isopropylacrylamide) Janus micromotors driven by simulated body fluid and blood plasma. *ACS Appl. Mater. Interfaces* 6:9897–903
83. Orozco J, Campuzano S, Kagan D, Zhou M, Gao W, Wang J. 2011. Dynamic isolation and unloading of target proteins by aptamer-modified microtransporters. *Anal. Chem.* 83:7962–69
84. Pak OS, Gao W, Wang J, Lauga E. 2011. High-speed propulsion of flexible nanowire motors: theory and experiments. *Soft Matter* 7:8169–81
85. Palacci J, Sacanna S, Steinberg AP, Pine DJ, Chaikin PM. 2013. Living crystals of light-activated colloidal surfers. *Science* 339:936–40
86. Palacci J, Sacanna S, Vatchinsky A, Chaikin PM, Pine DJ. 2013. Photoactivated colloidal dockers for cargo transportation. *J. Am. Chem. Soc.* 135:15978–81
87. Pantarotto D, Browne WR, Feringa BL. 2008. Autonomous propulsion of carbon nanotubes powered by a multienzyme ensemble. *Chem. Commun.* 2008:1533–35
88. Parry BR, Surovtsev IV, Cabeen MT, O'Hern CS, Dufresne ER, Jacobs-Wagner C. 2014. The bacterial cytoplasm has glass-like properties and is fluidized by metabolic activity. *Cell* 156:183–94
89. Patra D, Sengupta S, Duan W, Zhang H, Pavlick R, Sen A. 2013. Intelligent, self-powered, drug delivery systems. *Nanoscale* 5:1273–83
90. Patra D, Zhang H, Sengupta S, Sen A. 2013. Dual stimuli-responsive, rechargeable micropumps via "host–guest" interactions. *ACS Nano* 7:7674–79
91. Pavlick RA, Sengupta S, McFadden T, Zhang H, Sen A. 2011. A polymerization-powered motor. *Angew. Chem. Int. Ed.* 50:9374–77
92. Paxton WF, Baker PT, Kline TR, Wang Y, Mallouk TE, Sen A. 2006. Catalytically induced electrokinetics for motors and micropumps. *J. Am. Chem. Soc.* 128:14881–88

93. Paxton WF, Kistler KC, Olmeda CC, Sen A, St Angelo SK, et al. 2004. Catalytic nanomotors: autonomous movement of striped nanorods. *J. Am. Chem. Soc.* 126:13424–31
94. Peyer KE, Zhang L, Nelson BJ. 2013. Bio-inspired magnetic swimming microrobots for biomedical applications. *Nanoscale* 5:1259–72
95. Pokroy B, Epstein AK, Persson-Gulda MCM, Aizenberg J. 2009. Fabrication of bioinspired actuated nanostructures with arbitrary geometry and stiffness. *Adv. Mater.* 21:463–69
96. Pusey PN. 2011. Brownian motion goes ballistic. *Science* 332:802–03
97. Qian B, Montiel D, Bregulla A, Cichos F, Yang H. 2013. Harnessing thermal fluctuations for purposeful activities: the manipulation of single micro-swimmers by adaptive photon nudging. *Chem. Sci.* 4:1420–29
98. Reinmüller A, Oğuz EC, Messina R, Löwen H, Schöpe HJ, Palberg T. 2012. Colloidal crystallization in the quasi-two-dimensional induced by electrolyte gradients. *J. Chem. Phys.* 136:164505–10
99. Restrepo-Peréz L, Soler L, Martínez-Cisneros C, Sánchez S, Schmidt OG. 2014. Biofunctionalized self-propelled micromotors as an alternative on-chip concentrating system. *Lab Chip* 14:2914–17
100. Roberts AJ, Kon T, Knight PJ, Sutoh K, Burgess SA. 2013. Functions and mechanics of dynein motor proteins. *Nat. Rev. Molec. Cell Biol.* 14:713–26
101. Saha S, Golestanian R, Ramaswamy S. 2014. Clusters, asters, and collective oscillations in chemotactic colloids. *Phys. Rev. E* 89:062316
102. Sakaue T, Kapral R, Mikhailov AS. 2010. Nanoscale swimmers: hydrodynamic interactions and propulsion of molecular machines. *Eur. Phys. J. B* 75:381–87
103. Sanchez S, Solovev AA, Schulze S, Schmidt OG. 2011. Controlled manipulation of multiple cells using catalytic microbots. *Chem. Commun.* 47:698–700
104. Sanchez T, Welch D, Nicastro D, Dogic Z. 2011. Cilia-like beating of active microtubule bundles. *Science* 333:456–59
105. Sen A, Ibele M, Hong Y, Velegol D. 2009. Chemo and phototactic nano/microbots. *Faraday Discuss.* 143:15–27
106. Sengupta S, Dey KK, Muddana HS, Tabouillot T, Ibele ME, et al. 2013. Enzyme molecules as nanomotors. *J. Am. Chem. Soc.* 135:1406–14
107. Sengupta S, Ibele ME, Sen A. 2012. Fantastic voyage: designing self-powered nanorobots. *Angew. Chem. Int. Ed.* 51:8434–45
108. Sengupta S, Patra D, Rivera IO, Agrawal A, Dey KK, et al. 2014. Self-powered enzyme micropumps. *Nat. Chem.* 6:415–22
109. Sengupta S, Spiering MM, Dey KK, Duan W, Patra D, et al. 2014. DNA polymerase as a molecular motor and pump. *ACS Nano* 8:2410–18
110. Shah AS, Ben-Shahar Y, Moninger TO, Kline JN, Welsh MJ. 2009. Motile cilia of human airway epithelia are chemosensor. *Science* 325:1131–34
111. Shields AR, Fiser BL, Evans BA, Falvo MR, Washburn S, Superfine R. 2010. Biomimetic cilia arrays generate simultaneous pumping and mixing regimes. *PNAS* 107:15670–75
112. Sidorenko A, Krupenkin T, Taylor A, Fratzl P, Aizenberg J. 2007. Reversible switching of hydrogel-actuated nanostructures into complex micropatterns. *Science* 315:487–90
113. Sigrist-Nelson K. 1975. Dipeptide transport in isolated intestinal brush border membrane. *Biochim. Biophys. Acta* 394:220–26
114. Skou JC. 1957. The influence of some cations on an adenosine triphosphatase from peripheral nerves. *Biochim. Biophys. Acta* 23:394–401
115. Skou JC. 1965. Enzymatic basis for active transport of Na^+ and K^+ across cell membrane. *Physiol. Rev.* 45:596–617
116. Sleigh MA, Aiello E. 1972. The movement of water by cilia. *Acta Protozool.* 11:265–77
117. Solomentsev Y, Anderson JL. 1994. Electrophoresis of slender particles. *J. Fluid Mech.* 279:197–215
118. Solovev AA, Mei Y, Bermúdez Ureña E, Huang G, Schmidt OG. 2009. Catalytic microtubular jet engines self-propelled by accumulated gas bubbles. *Small* 5:1688–92
119. Solovev AA, Sanchez S, Pumera M, Mei YF, Schmidt OG. 2010. Magnetic control of tubular catalytic microbots for the transport, assembly, and delivery of micro-objects. *Adv. Funct. Mater.* 20:2430–35
120. Spudich J, Rice SE, Rock RS, Purcell TJ, Warrick HM. 2011. Optical traps to study properties of molecular motors. *Cold Spring Harb. Protoc.* 11:1305–18

121. Stock C, Heureux N, Browne WR, Feringa BL. 2008. Autonomous movement of silica and glass microobjects based on a catalytic molecular propulsion system. *Chem. Eur. J.* 14:3146–53
122. Sundararajan S, Sengupta S, Ibele ME, Sen A. 2010. Drop-off of colloidal cargo transported by catalytic Pt–Au nanomotors via photochemical stimuli. *Small* 6:1479–82
123. Tottori S, Zhang L, Qiu F, Krawczyk KK, Franco-Obregón A, Nelson BJ. 2012. Magnetic helical micromachines: fabrication, controlled swimming, and cargo transport. *Adv. Mater.* 24:811–16
124. van Oosten CL, Bastiaansen CWM, Broer DJ. 2009. Printed artificial cilia from liquid-crystal network actuators modularly driven by light. *Nat. Mater.* 8:677–82
125. Vilfan M, Potočnik A, Kavčič B, Osterman N, Poberaj I, et al. 2010. Self-assembled artificial cilia. *PNAS* 107:1844–47
126. Wang H, Zhao G, Pumera M. 2013. Blood electrolytes exhibit a strong influence on the mobility of artificial catalytic microengines. *Phys. Chem. Chem. Phys.* 15:17277–80
127. Wang J, Gao W. 2012. Nano/microscale motors: biomedical opportunities and challenges. *ACS Nano* 6:5745–51
128. Wang N, Butler JP, Ingber DE. 1993. Mechanotransduction across the cell surface and through the cytoskeleton. *Science* 260:1124–27
129. Wang W, Castro LA, Hoyos M, Mallouk TE. 2012. Autonomous motion of metallic microrods propelled by ultrasound. *ACS Nano* 6:6122–32
130. Wang W, Duan W, Ahmed S, Mallouk TE, Sen A. 2013. Small power: autonomous nano- and micromotors propelled by self-generated gradients. *Nano Today* 8:531–54
131. Wang W, Duan W, Sen A, Mallouk TE. 2013. Catalytically powered dynamic assembly of rod-shaped nanomotors and passive tracer particles. *PNAS* 110:17744–49
132. Wang W, Li S, Mair L, Ahmed S, Huang TJ, Mallouk TE. 2014. Acoustic propulsion of nanorod motors inside living cells. *Angew. Chem.* 126:3265–68
133. Wang Y, Gao Y, Wyss H, Anderson P, den Toonder J. 2013. Out of the cleanroom, self-assembled magnetic artificial cilia. *Lab Chip* 13:3360–66
134. Wheat PM, Marine NA, Moran JL, Posner JD. 2010. Rapid fabrication of bimetallic spherical motors. *Langmuir* 26:13052–55
135. Wong T-S, Kang SH, Tang SKY, Smythe EJ, Hatton BD, et al. 2011. Bioinspired self-repairing slippery surfaces with pressure-stable omniphobicity. *Nature* 477:443–47
136. Wu J, Balasubramanian S, Kagan D, Manesh KM, Campuzano S, Wang J. 2010. Motion-based DNA detection using catalytic nanomotors. *Nat. Commun.* 1:36
137. Yadav V, Freedman JD, Grinstaff M, Sen A. 2013. Bone-crack detection, targeting and repair using ion gradients. *Angew. Chem. Int. Ed.* 52:10997–1001
138. Yadav V, Pavlick RA, Meckler SM, Sen A. 2014. Triggered detection and deposition: toward the repair of microcracks. *Chem. Mater.* 26:4647–52
139. Yadav V, Zhang H, Pavlick R, Sen A. 2012. Triggered "on/off" micropumps and colloidal photodiode. *J. Am. Chem. Soc.* 134:15688–91
140. Zhang H, Duan W, Liu L, Sen A. 2013. Depolymerization-powered autonomous motors using biocompatible fuel. *J. Am. Chem. Soc.* 135:15734–37
141. Zhang H, Duan W, Lu M, Zhao X, Shklyaev S, et al. 2014. Self-powered glucose-responsive micropumps. *ACS Nano* 8:8537–42
142. Zhang H, Yeung K, Robbins JS, Pavlick RA, Wu M, et al. 2012. Self-powered microscale pumps based on analyte-initiated depolymerization reactions. *Angew. Chem. Int. Ed.* 51:2400–4
143. Zhang L, Peyer KE, Nelson BJ. 2010. Artificial bacterial flagella for micromanipulation. *Lab Chip* 10:2203–15
144. Zhao G, Wang H, Khezri B, Webster RD, Pumera M. 2013. Influence of real-world environments on the motion of catalytic bubble-propelled micromotors. *Lab Chip* 13:2937–41